Tuning of metal work functions with self-assembled monolayers

de Boer, B; Hadipour, A; Mandoc, MM; van Woudenbergh, T; Blom, PWM

Published in:
Advanced Materials

DOI:
10.1002/adma.200401216

Publication date:
2005

[5] A. Aggeli, M. Bell, N. Boden, J. N. Keen, P. F. Knowles, T. C. B. McLeish, M. Pitkeathly, S. E. Radford, *Nature* **1997**, *386*, 259.
[6] W. Shenton, S. A. Davis, S. Mann, *Adv. Mater.* **1999**, *11*, 449.
[7] S. Connolly, D. Fitzmaurice, *Adv. Mater.* **1999**, *11*, 1202.
[8] a) J. Yang, M. Mayer, J. K. Kriebel, P. Garstecki, G. M. Whitesides, *Angew. Chem. Int. Ed.* **2004**, *43*, 1555. b) H. Zhang, Z. Li, C. A. Mirkin, *Adv. Mater.* **2002**, *14*, 1472.
[9] For similar work where structural features of bacteria have been used to control nanoparticle assembly, see W. Shenton, D. Pum, U. B. Sleytr, S. Mann, *Nature* **1997**, *389*, 585.
[10] S. W. Chen, *Anal. Chim. Acta* **2003**, *496*, 29.
[11] F. X. Redl, K. S. Cho, C. B. Murray, S. O'Brien, *Nature* **2003**, *423*, 968.
[12] A. K. Boal, F. Ilhan, J. E. DeRouchey, T. Thurn-Albrecht, T. P. Russell, V. M. Rotello, *Nature* **2000**, *404*, 746.
[13] N. O. Fischer, C. M. McIntosh, J. M. Simard, V. M. Rotello, *Proc. Natl. Acad. Sci. USA* **2002**, *99*, 5018.
[14] C. D. Keating, K. M. Kovaleski, M. J. Natan, *J. Phys. Chem. B* **1998**, *102*, 9404.
[15] N. Ui, *Biochim. Biophys. Acta* **1971**, *229*, 582.
[16] G. H. Barlow, E. Margolia, *J. Biol. Chem.* **1966**, *241*, 1473.
[17] The electrostatic repulsion from CC is expected to be analogous to other charged-colloid systems where similarly charged nanoparticles electrostatically repel each other. For analogous colloid systems, see T. H. Galow, A. K. Boal, V. M. Rotello, *Adv. Mater.* **2000**, *12*, 576.
[18] N. Sreerama, R. W. Woody, *Anal. Biochem.* **2000**, *287*, 252.
[19] J. B. Carroll, B. L. Frankamp, S. Srivastava, V. M. Rotello, *J. Mater. Chem.* **2004**, *14*, 690.
[20] A. Lobley, L. Whitmore, B. A. Wallace, *Bioinformatics* **2002**, *18*, 211.
[21] A. Lobley, B. A. Wallace, *Biophys. J.* **2001**, *80*, 373A.

Tuning of Metal Work Functions with Self-Assembled Monolayers**

By *Bert de Boer*,* *Afshin Hadipour*, *M. Magdalena Mandoc*, *Teunis van Woudenbergh*, and *Paul W. M. Blom*

Metallic contacts in organic optoelectronic devices are determinative of their ultimate performance.[1] Preparation methods, diffusion of metal atoms, reactivity of the metal toward air and organic materials,[2] and roughness of the metallic contact can have a detrimental influence on the stability and performance of organic thin-film devices like light-emitting diodes (LEDs), photovoltaic (PV) cells, and (ambipolar) field-effect transistors (FETs). Although these influences have to be addressed before a reliable and reproducible device can be produced, one first has to take into account the intrinsic properties of the metal, like its transparency, reactivity, and especially for (opto)electronic applications, its work function.

For efficient electron and hole injection into polymer LEDs, the work function of the electrode has to match (within a few tenths of an eV) the energy level of the lowest unoccupied molecular orbital (LUMO) or highest occupied molecular orbital (HOMO) of the polymer layer, respectively.[1,3] In conjugated polymer/fullerene-based solar cells, the experimental open-circuit voltage (V_{OC}) for non-ohmic contacts is determined by the difference in the work functions of the electrodes. For ohmic contacts, the V_{OC} is governed by the HOMO and LUMO levels of the acceptor and donor, respectively.[4] For ambipolar FETs, the main difficulty is achieving injection of both electrons and holes in the organic semiconductor from the same electrode, since the work function will always result in an injection barrier of at least half of the bandgap for one of the carriers.[5] Facilitating the charge injection improves the device performance and tuning the work function of the metal to match the HOMO (or valence band) and/or LUMO (conducting band) is desirable. Obviously, the performances of all the devices mentioned above are determined by the work functions of their metal electrodes.

As demonstrated by several authors, tuning of the metal work function (Φ_M) can be accomplished by using polar molecules that can self-assemble on the metal and form a highly ordered, thin, two-dimensional (2D) layer which has a dipole in the desired direction (Fig. 1).[6–19] Alkanethiols (Fig. 1B) and perfluorinated alkanethiols (Fig. 1C) are known to form such self-assembled monolayers (SAMs)[6,12,14–16,20–22] on group Ib and group VIII metals. Since alkanethiols and perfluorinated alkanethiols have opposite dipoles, they can be used to, respectively, decrease[6,8,14,16] and increase[6,12] the work functions of metals (i.e., shift the vacuum energy levels[23] in Fig. 1). In addition, conjugated mono- and dithiols are known to form highly ordered SAMs on metals surfaces,[24] which

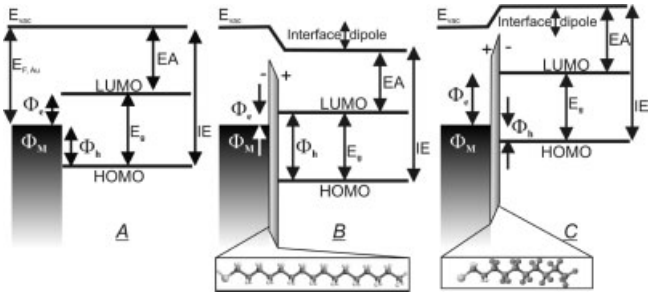

Figure 1. Schematic energy-level diagrams of metal/organic interfaces with metal work function, Φ_M, located within the HOMO–LUMO gap (E_g) of the organic semiconductor. A) Electron injection barrier (Φ_e) and hole-injection barrier (Φ_h) for an untreated interface (without SAM). B) Alkanethiols impose an interface dipole that decreases Φ_e and increases Φ_h. C) 1H,1H,2H,2H-perfluoroalkanethiols impose an interface dipole that increases Φ_e and decreases Φ_h. + and – depict the direction of the interface dipole. $E_{F,Au}$: Fermi energy of Au; E_{vac}: local vacuum energy level; *IE*: ionization energy; *EA*: electron affinity.

[*] Dr. B. de Boer, A. Hadipour, M. M. Mandoc, T. van Woudenbergh, Prof. P. W. M. Blom
Molecular Electronics, Materials Science Centre
University of Groningen
Nijenborgh 4, NL-9747 AG, Groningen (The Netherlands)
E-mail: b.de.boer@phys.rug.nl

[**] We acknowledge Mark-Jan Spijkman, Remco Foekema, Jur Wildeman and Minte Mulder for their assistance. The work of MMM and TvW forms part of the research program of the Dutch Polymer Institute (#323, #275).

DOI: 10.1002/adma.200401216

ADVANCED MATERIALS

makes them particularly interesting for use in optoelectronic devices.[7,8] Besides using the dipoles of SAMs to tune metal work functions, Kobayashi and co-workers also demonstrated recently that the interface dipole formed by SAMs can control the charge-carrier density in organic FETs.[25]

In this work, the tuning of metal work functions (Φ_M) using SAMs is described and we demonstrate that the work function of a silver electrode can be tuned from 3.8 to 5.5 eV using two different SAMs. Consequently, the hole-injection barrier of Ag ($\Phi_{Ag} = 4.4$ eV) with poly(2-methoxy-5-(2′-ethylhexyloxy)–1,4-phenylene vinylene) (MEH–PPV) can be completely eliminated resulting in an ohmic contact, or increased to such an extent that the current densities between the two modified electrodes differs by 6 orders of magnitude at a 5 V bias. The latter allows the electron-only current to be measured in a polymer/polymer blend solar cell.

One can consider a SAM based on alkanethiols to be a dipole layer in which the total dipole moment arises of two internal dipoles stacked on top of each other. The first effective dipole is formed by the metal–sulfur (M–S) charge-transfer interaction, and the second effective dipole is determined by the composition of the monolayer itself. The total effective dipole at a metal surface can be visualized as a double layer of two parallel charge sheets with a charge density, σ ($= Nq$, N = grafting density; q = unit charge), which are separated by two dielectric layers of thicknesses l_{M-S} and l_{SAM}, with dielectric constants of κ_{M-S} and κ_{SAM}, respectively. From classical electrostatics, one can calculate the potential drop caused by the dipole from the integral of the electric fields across the parallel sheets.[8] The change in work function can be written as:

$$\Delta\phi = -N\left[\frac{\mu_{\perp,SAM}}{\varepsilon_0\kappa_{SAM}} + \frac{\mu_{M-S}}{\varepsilon_0\kappa_{M-S}}\right] \quad (1)$$

where the first term represents the effective dipole moment (vector perpendicular to the surface) of the monolayer, and the second term takes into account the effective intrinsic M–S dipole created by the metal surface, which is chemically modified with the thiolate end group of the SAM ($\mu_{\perp,SAM}$: dipole moment of the SAM perpendicular to the surface; ε_0: permittivity of free space). The effective M–S dipole ($\mu_{M-S}/\varepsilon_0\kappa_{M-S}$) is assumed to be almost independent of the alkane chain length and composition, but strongly dependent on the nature of the metal.

For alkanethiol SAMs, the effective M–S dipole has an opposite, but smaller value than the effective dipole of the SAM itself, which results in a smaller shift of the work function when compared to the perfluorinated alkanethiols. The latter exhibits an effective M–S dipole in the same direction as that of the monolayer. Furthermore, the M–S dipole depends on the kind of metal used. In this work, we demonstrate that the silver–sulfur dipole is larger than the gold–sulfur dipole.

The grafting density of the SAMs on a metal depends on the commensurate, close-packed structure of the SAM on that metal. Alkanethiols adopt the commensurate $(\sqrt{3} \times \sqrt{3})$ R30° (following the Wood's notation) hexagonal lattice on Au(111) with an approximate off-normal tilt, α, of 30° and a nearest-neighbor distance of 4.97 Å.[26] The sulfur head group occupies the threefold hollow sites of the Au(111) surface. This results in a value of N of 4.6×10^{18} m^{-2} on Au (111). For alkanethiols on Ag, the chains are oriented closer to the normal axis ($\alpha \sim 12°$),[27] due to the larger nearest-neighbor spacing in the (111) plane for Ag (2.89 Å versus 2.88 Å for Au[28]), but the grafting density of alkanethiols on Ag is the same as on Au ($N = 4.6 \times 10^{18}$ m^{-2}). This implies that only the difference in the tilt angles of the SAM for Au (30°) and Ag (12°) will result in a change of about 11 % in the effective dipole moment perpendicular to the metal surface, since the effective dipole moment is given by: $\mu_{\perp,SAM} = \mu_{molecule}\cos\alpha$.

Perfluorinated alkanethiols on Au (111) probably adopt a commensurate high-order c(7 × 7) (c: centered structure, following the Wood's notation) superlattice of close-packed molecules with a lattice constant of 5.8 ± 0.1 Å.[20,21,29] Although a commensurate p(2 × 2)[29] (p: primitive structure, following the Wood's notation) or an incommensurate lattice[20] were also reported, the nearest-neighbor distance is ~5.8 Å. The tilt angle of perfluorinated alkanethiols is lower than that for alkanethiols, namely about 12–20°.[20,29] This results in a grafting density for 1*H*,1*H*,2*H*,2*H*-perfluoroalkanethiols of 3.4×10^{18} m^{-2} on Au (111). Although data on the tilt angle of perfluorinated alkanethiols on Ag is not available, we expect similar behavior to that of perfluorinated alkanethiols on Au. The tilt angle is expected to be closer to the surface normal, since Ag has a slightly larger nearest neighbor spacing in the (111) plane than Au, and the grafting density for 1*H*,1*H*,2*H*,2*H*-perfluoroalkanethiols is estimated to be 3.4×10^{18} m^{-2} on Ag. Since the grafting density is the same on Ag and Au, and the tilt angles are very small (< 20°) for both metals, this SAM is expected to give almost the same shift in work function (not taking into account the M–S dipole) for both Au and Ag (< 5 %). An overview of the properties, and the calculated and measured work-function shifts of the SAMs on a particular metal surface is given in Table 1.

Figure 2 displays the work functions of 20 nm Ag layers (unmodified and modified with SAMs) on glass, measured using a Kelvin probe under a N_2 atmosphere. The work functions measured were stable for at least 5 days. The modifica-

Table 1. Overview of properties of SAMs on Au and Ag.

	κ_{SAM}	N [m^{-2}]	a [°]	$\mu_{\perp,SAM}$ [b] [D]	$\Delta\Phi_{calc}$ [c] [eV]	$\Delta\Phi_{meas}$ [d] [eV]
Au-$SC_{16}H_{33}$	2.5	4.6×10^{18}	35	1.60	–1.0	–0.8
Au-$SC_2H_4C_8F_{17}$	2.1 [a]	3.4×10^{18}	16	2.19	1.3	0.6
Ag-$SC_{16}H_{33}$	2.5	4.6×10^{18}	12	1.91	–1.3	–0.6
Ag-$SC_2H_4C_8F_{17}$	2.1 [a]	3.4×10^{18}	8	2.25	1.4	1.1

[a] Dielectric constant taken from poly(tetrafluoroethylene) (PTFE) [30]. [b] Dipole moment of the SAM corrected for the tilt angle. The dipole moment was calculated for unbound, isolated molecules with a thiol end group (see Experimental). [c] Work-function shifts calculated from Equation 1 and excluding the M–S dipole. [d] Work-function shifts measured with Kelvin probe.

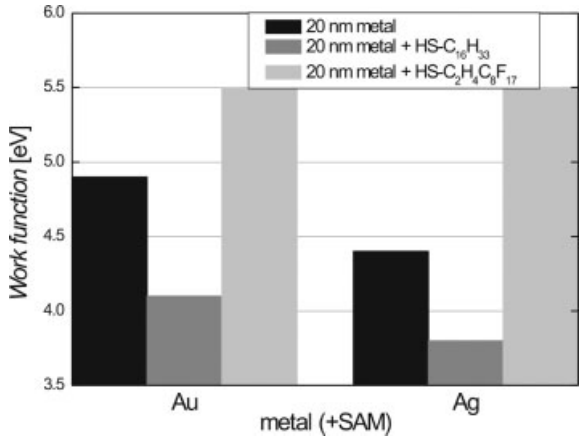

Figure 2. Work function of as-deposited Au, Ag, and Au and Ag modified by self-assembled monolayers of hexadecanethiol, and 1*H*,1*H*,2*H*,2*H*-perfluorodecanethiol.

tion was performed by two SAMs of opposing dipoles, namely 1*H*,1*H*,2*H*,2*H*-perfluorodecanethiol and hexadecanethiol. A large increase of Φ is observed when Ag was modified with a SAM of 1*H*,1*H*,2*H*,2*H*-perfluorodecanethiol, resulting in a work function of 5.5 eV that slowly stabilized at 5.4 eV. Compared to silver (4.4 eV), we were able to increase Φ by 1.1 eV. Alternatively, modification of silver with a self-assembled monolayer of hexadecanethiol lowered Φ by 0.6 eV to 3.8 eV (Fig. 2).

Similarly, we prepared Au-coated (20 nm) substrates without and with SAMs of 1*H*,1*H*,2*H*,2*H*-perfluorodecanethiol and hexadecanethiol. We measured Φ for the untreated gold to be 4.9 eV, whereas the SAMs of 1*H*,1*H*,2*H*,2*H*-perfluorodecanethiol and hexadecanethiol shifted Φ to 5.5 eV and 4.1 eV, respectively (Fig. 2). Apparently, the interface-dipole formation of the perfluorinated alkanethiol on Au is less efficient than on Ag, whereas the opposite is true for the alkanethiol. This difference can not be attributed to the difference in tilt angle of the SAMs on Au and Ag (Table 1). Alkanethiols have a tilt angle of ~30° on Au, whereas on Ag the chains are closer to the normal axis (~12°),[27] due to the larger nearest-neighbor spacing in the (111) plane for Ag. Similarly, the tilt angle for perfluorinated alkanethiols on Ag is assumed to be smaller than the tilt angle on Au (~15°). This relatively small difference in tilt angle on Ag can therefore only account for a small increase in the interface dipole perpendicular to the metal surface (~11 % for alkanethiol and ~5 % for perfluorinated alkanethiols). However, more important by far is the contribution of the M–S effective dipole to the overall work-function shift. As mentioned before, the M–S dipole moment has the same sign as the dipole moment of the perfluorinated alkanethiol and an opposite sign to that of hexadecanethiol. Since the work-function shift of the perfluorinated alkanethiol is larger on Ag than on Au, and the work-function shift of hexadecanethiol is smaller for Ag than for Au (Fig. 2), it is evident that the Ag–S dipole moment is larger than the Au–S dipole moment.

An important issue is to check whether these strong work-function shifts are also reflected in the performance of devices when SAM-modified electrodes are used. In injection-limited polymer LEDs, in which a semitransparent Ag electrode is used as the hole-injection contact and MEH–PPV (chemical structure is presented in Fig. 3A) as the active polymer, a hole-injection barrier of typically ~0.9 eV exists due to the energy mismatch of the HOMO of MEH–PPV (5.3 eV) and the work function of Ag (4.4 eV).[3] Since the work function of Ag could be enhanced by 1.1 eV using a SAM of 1*H*,1*H*,2*H*,2*H*-perfluorodecanethiol, it should, in principle, be possible to change the charge-transport properties from being heavily injection limited (Ag) to bulk space-charge limited (Ag/SAM). For this purpose we made an LED based on MEH–PPV with the configuration glass/Ag/$HSC_2H_4C_8F_{17}$/

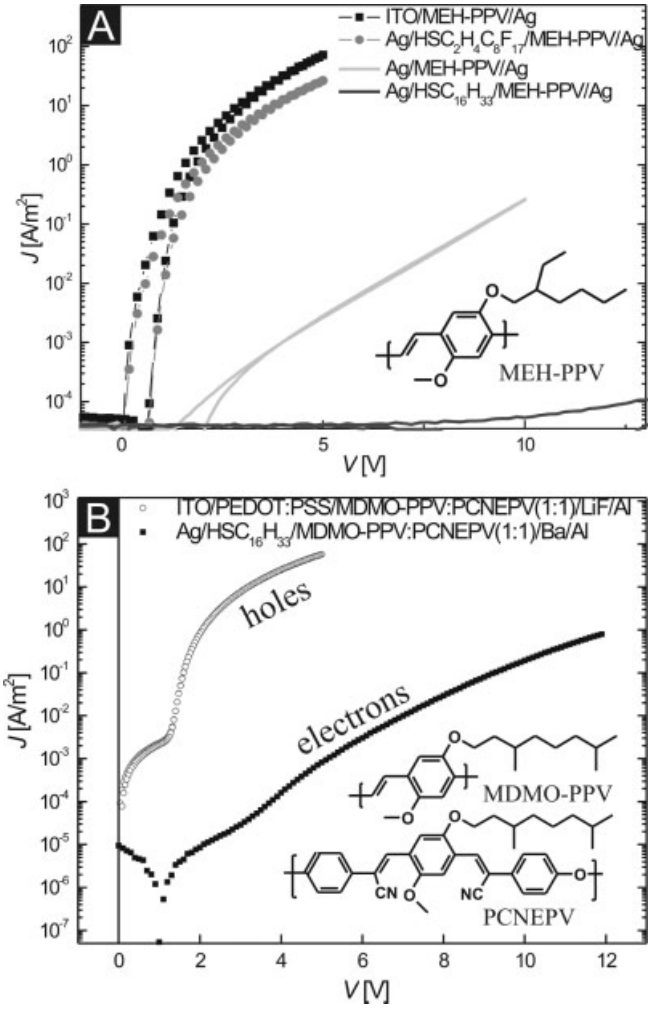

Figure 3. A) Current-density–voltage characteristics of diodes based on MEH–PPV. The hole-injection electrode was modified to be: ITO, Ag with 1*H*,1*H*,2*H*,2*H*-perfluorodecanethiol, unmodified Ag, and Ag with hexadecanethiol. B) Current-density–voltage characteristics under dark conditions for a solar cell based on MDMO–PPV and PCNEPV (1:1) with PEDOT:PSS and LiF/Al electrodes, and with Ag/$HSC_{16}H_{33}$ and Ba/Al electrodes.

ADVANCED MATERIALS

MEH–PPV/Ag. Since we are interested in the hole-injection barrier, all LEDs had a top contact of silver that blocked the electron injection. As a reference, LEDs without an SAM and one with $C_{16}H_{33}SH$ (which lowered the work function of Ag and further increased the injection barrier) (Fig. 3A) were also fabricated. Usually, indium tin oxide (ITO) and/or PEDOT/PSS are used as electrodes in MEH–PPV-based LEDs, because both are known to form ohmic contacts with MEH–PPV. For comparison, an LED based on an ohmic ITO contact (ITO/MEH–PPV/Ag) was also made (Fig. 3A). From Figure 3A, it appears that the current-density–voltage (*J*–*V*) characteristics of the device based on Ag modified with 1*H*,1*H*,2*H*,2*H*-perfluorodecanethiol is nearly identical to the ITO-based bulk-limited device. As expected, the effective dipole created by the perfluorinated SAM shifted the work function of the Ag electrode by about 1 eV, thereby eliminating the hole-injection barrier and creating an ohmic contact for hole injection with MEH–PPV. The LED with an unmodified Ag hole-injection contact exhibited a contact-energy barrier of typically ~0.9 eV due to the work function of Ag (4.4 eV), resulting in a current density that was an order of magnitude lower. The hole current is even more suppressed by the Ag electrode modified with hexadecanethiol. As demonstrated above, the effective dipole created by this SAM lowered the work function of Ag to 3.8 eV, creating an energy barrier of ~1.5 eV with respect to the HOMO of MEH–PPV. This modification clearly increased the energy barrier for hole injection (Fig. 3A), suppressing the hole current almost completely.

The ability to completely suppress the injection of one kind of charge carrier is a very attractive tool for the characterization of charge transport in composite materials, as used in, for example, PV devices. In many conjugated polymers, charge transport is mainly dominated by holes.[31] Consequently, the dark current of solar cells based on a polymer/polymer blend will be dominated by the holes in the donor polymer, making it difficult to extract information about the electron transport in the acceptor polymer inside the blend. As an example, the dark-current densities of a PEDOT:PSS/MDMO–PPV:PCNEPV(1:1)/LiF/Al (where MDMO is 2-methoxy-5-(3′,7′-dimethyloctyloxy) and PCNEPV is poly[oxa-1,4-phenylene-(1-cyano-1,2-vinylene)-(2-methoxy-5-(3′,7′-dimethyloctyloxy)-1,4-phenylene)-1,2-(2-cyanovinylene)-1,4-phenylene]; chemical structure is presented in Fig. 3B) device and a Ag/$HSC_{16}H_{33}$/MDMO–PPV:PCNEPV(1:1)/Ba/Al device are shown in Figure 3B. The PCNEPV is known to have a low reduction potential (LUMO at 3.52 eV) due to the high electron affinity of the cyano groups. Therefore, PCNEPV is used in polymer/polymer solar cells as the electron accepting and transporting material.[32,33] The observed dark current of a conventional PV cell with a PEDOT:PSS bottom electrode is completely dominated by the holes in the PPV since the hole current is orders of magnitude higher than the electron current. However, when a Ag/$HSC_{16}H_{33}$ bottom electrode (with $\Phi = 3.8$ eV) is employed, a large hole-injection barrier is created (~1.5 eV) and the hole current in the PPV can be completely blocked (Figs. 1B, 3A). The resulting dark current now stems from the electron transport in the PCNEPV (Fig. 3B). Thus, apart from improving charge injection, SAM-modified electrodes are also very useful in selectively blocking one type of charge carrier in optoelectronic devices. In this manner, the electron-only currents can be measured in pristine polymers or in polymer/polymer blends without having to spin-coat them onto highly reactive bottom contacts like Ca or Ba.[34]

In conclusion, we have demonstrated the tuning of metal work functions by chemically modifying the metal surfaces through the formation of chemisorbed SAMs derived from 1*H*,1*H*,2*H*,2*H*-perfluorinated alkanethiols and hexadecanethiol. The ordering inherent in the SAMs creates an effective, molecular dipole at the metal/SAM interface, which increased the work function of Ag (Φ_{Ag} ~4.4 eV) to 5.5 eV ($\Delta\Phi$ ~1.1 eV) for 1*H*,1*H*,2*H*,2*H*-perfluorinated alkanethiols. Hexadecanethiol, on the other hand, shifted Φ_{Ag} to 3.8 eV ($\Delta\Phi$ ~0.6 eV). On Au, the SAM of 1*H*,1*H*,2*H*,2*H*-perfluorodecanethiol raised Φ_{Au} (4.9 eV) by 0.6 eV to 5.5 eV, whereas hexadecanethiol decreased Φ_{Au} by 0.8 eV. These chemically modified electrodes were used in polymer LEDs and hole injection into MEH–PPV was investigated. An ohmic contact for hole injection between a silver electrode functionalized with the perfluorinated SAMs and MEH–PPV, with a HOMO of 5.3 eV, was established. Conversely, a SAM of hexadecanethiol lowered Φ_{Ag} of a silver electrode to 3.8 eV, and blocked hole injection into PPV, which enabled studying the electron transport in composite devices. The electron-only current was measured in a polymer/polymer blend PV cell based on MDMO–PPV and PCNEPV. This method demonstrates a simple and attractive approach to modify and improve metal/organic contacts in organic electronic devices like LEDs, PV cells, and FETs.

Experimental

The perfluorinated alkanethiols ($C_6F_{13}C_2H_4$–SH, $C_8H_{17}C_2H_4$–SH) were synthesized according to a previously reported method [35]. These compounds were readily obtained in high yields. Hexadecanethiol (Aldrich) was distilled prior to use. Poly(2-methoxy-5-(2′-ethylhexyloxy)–1,4-phenylene vinylene) (MEH–PPV) was synthesized via the Gilch method [36]. Poly[2-methoxy-5-(3′,7′-dimethyloctyloxy)–1,4-phenylene vinylene] (MDMO–PPV) and poly[oxa-1,4-phenylene-(1-cyano-1,2-vinylene)-(2-methoxy-5-(3′,7′-dimethyloctyloxy)-1,4-phenylene)-1,2-(2-cyanovinylene)-1,4-phenylene] (PCNEPV) [33] (chemical structures are given in Fig. 3B) were kindly provided by TNO, Eindhoven, The Netherlands. Glass slides and ITO substrates were thoroughly cleaned with soap/water, rinsed with copious amount of Millipore water, ultrasonically cleaned with acetone and 2-propanol, and dried in an oven at 120 °C. Prior to metal-vapor deposition, the substrates were UV-ozone treated for 20 min. Metal-coated substrates were prepared by vapor-depositing silver or gold (200–500 Å thickness) on cleaned glass slides or ITO substrates. The self-assembly was performed by immersing the substrates into a ~3×10^{-3} M solution of alkanethiol in ethanol (in a N_2-purged glove box). Immediately after deposition of the metal layer, the gold or silver substrates were immersed into the SAM solution for at least 2 days without exposure to ambient. The substrates were thoroughly rinsed with ethanol, toluene, and 2-propanol, dried with a N_2 flow, and immediately measured or

used for the fabrication of LEDs or solar cells. The reference solar cell devices in this study were prepared using ITO-coated glass substrates. To supplement this bottom electrode, a hole-transport layer of PEDOT:PSS (Bayer AG) was spin-coated from an aqueous dispersion solution, under ambient conditions, before drying the substrates at 140 °C. Next, composite layers of MDMO–PPV and PCNEPV were spin-coated from a chlorobenzene solution on top of the PEDOT:PSS layer, with film thicknesses of 210 nm. To complete the solar-cell devices, 1 nm lithium fluoride (LiF) or 5 nm Ba topped with aluminum (Al, 100 nm) electrodes were deposited by thermal evaporation under vacuum (1×10^{-7} mbar; 1 mbar = 100 Pa).

The Kelvin probe was calibrated with freshly cleaved highly oriented pyrolytic graphite (HOPG) in a nitrogen atmosphere (glove box). Freshly cleaved HOPG is known to have a stable work function of 4.48 eV [37].

The dipole moments were calculated (HyperChem 6.03) using a geometry optimization with molecular mechanic force field MM^+, Polak-Ribiere (RMS gradient 0.05 kcal $Å^{-1}$ mol^{-1}), followed by a geometry optimization with the semi-empirical PM3 method (Polak-Ribiere, RMS gradient 0.05 kcal $Å^{-1}$ mol^{-1}). In this geometry the dipole moment was calculated. The dipole moments of the molecules were calculated for the unbound, isolated (gas phase) molecules (with –SH end groups). Upon adsorption, the effective dipole moment of the molecule and its optimized geometry could have changed due to the Au–S interaction.

LEDs were prepared by spin-coating MEH–PPV from toluene (40 mg MEH–PPV per 10 mL toluene, dissolved at 60 °C) onto the freshly prepared substrates in a N_2-atmosphere (layer thickness ~150 nm). Subsequently, a 50 nm Ag top electrode was vapor-deposited at a pressure $< 2 \times 10^{-6}$ mbar. Current-density–voltage (*J–V*) measurements were performed under an N_2 atmosphere in the dark (< 1 ppm O_2 and < 1 ppm H_2O) using a computer-controlled source measure unit Keithley 2400.

Received: July 27, 2004
Final version: October 22, 2004

[1] T. van Woudenbergh, P. W. M. Blom, J. N. Huiberts, *Appl. Phys. Lett.* **2003**, *82*, 985.
[2] B. de Boer, M. M. Frank, Y. J. Chabal, W. Jiang, E. Garfunkel, Z. Bao, *Langmuir* **2004**, *20*, 1539.
[3] T. van Woudenbergh, P. W. M. Blom, M. C. J. M. Vissenberg, J. N. Huiberts, *Appl. Phys. Lett.* **2001**, *79*, 1697.
[4] a) V. D. Mihailetchi, P. W. M. Blom, J. C. Hummelen, M. T. Rispens, *J. Appl. Phys.* **2003**, *94*, 6849. b) J. K. J. van Duren, V. D. Mihailetchi, P. W. M. Blom, T. van Woudenbergh, J. C. Hummelen, M. T. Rispens, R. A. J. Janssen, M. M. Wienk, *J. Appl. Phys.* **2003**, *94*, 4477.
[5] E. J. Meijer, D. M. de Leeuw, S. Setayesh, E. van Veenendaal, B.-H. Huisman, P. W. M. Blom, J. C. Hummelen, U. Scherf, T. M. Klapwijk, *Nat. Mater.* **2003**, *2*, 678.
[6] I. H. Campbell, S. Rubin, T. A. Zawodzinski, J. D. Kress, R. L. Martin, D. L. Smith, N. N. Barashkov, J. P. Ferraris, *Phys. Rev. B* **1996**, *54*, 14 321.
[7] I. H. Campbell, J. D. Kress, R. L. Martin, D. L. Smith, N. N. Barashkov, J. P. Ferraris, *Appl. Phys. Lett.* **1997**, *71*, 3528.
[8] R. W. Zehner, B. F. Parsons, R. H. Hsung, L. R. Sita, *Langmuir* **1999**, *15*, 1121.
[9] B. Choi, J. Rhee, H. H. Lee, *Appl. Phys. Lett.* **2001**, *79*, 2109.
[10] A. Vilan, D. Cahen, *Trends Biotechnol.* **2002**, *20*, 22.
[11] G. Ashkenasy, D. Cahen, R. Cohen, A. Shanzer, A. Vilan, *Acc. Chem. Res.* **2002**, *35*, 121.
[12] D. M. Alloway, M. Hofmann, D. L. Smith, N. E. Gruhn, A. L. Graham, R. Colorado, Jr., V. H. Wysocki, T. R. Lee, P. A. Lee, N. R. Armstrong, *J. Phys. Chem. B* **2003**, *107*, 11 690.
[13] S. C. Veenstra, A. Heeres, G. Hadziioannou, G. A. Sawatzky, H. T. Jonkman, *Appl. Phys. A* **2002**, *75*, 661.
[14] S. D. Evans, A. Ulman, *Chem. Phys. Lett.* **1990**, *170*, 462.
[15] J. Lü, E. Delamarche, L. Eng, R. Bennewitz, E. Meyer, H.-J. Güntherodt, *Langmuir* **1999**, *15*, 8184.
[16] S. D. Evans, E. Urankar, A. Ulman, N. Ferris, *J. Am. Chem. Soc.* **1991**, *113*, 4121.
[17] S. Howell, D. Kuila, B. Kasibhatla, C. P. Kubiak, D. Janes, R. Reifenberger, *Langmuir* **2002**, *18*, 5120.
[18] a) M. Bruening, R. Cohen, J. F. Guillemoles, T. Moav, J. Libman, A. Sahnzer, D. Cahen, *J. Am. Chem. Soc.* **1997**, *119*, 5720. b) D. Cahen, A. Kahn, *Adv. Mater.* **2003**, *15*, 271.
[19] F. Nüesch, M. Carrara, L. Zuppiroli, *Langmuir* **2003**, *19*, 4871.
[20] G.-Y. Liu, P. Fenter, C. E. D. Chidsey, D. F. Ogletree, P. Eisenberger, M. Salmeron, *J. Chem. Phys.* **2000**, *101*, 4301.
[21] K. Tamada, T. Ishida, W. Knoll, H. Fukushima, R. Collorado, Jr., M. Graupe, O. E. Shmakova, T. R. Lee, *Langmuir* **2001**, *17*, 1913.
[22] H. Schönherr, G. J. Vancso, *Langmuir* **1997**, *13*, 3769.
[23] H. Ishii, K. Sugiyama, E. Ito, K. Seki, *Adv. Mater.* **1999**, *11*, 605.
[24] B. de Boer, H. Meng, D. F. Perepichka, J. Zheng, M. M. Frank, Y. J. Chabal, Z. Bao, *Langmuir* **2003**, *19*, 4272.
[25] S. Kobayashi, T. Nishikawa, T. Takenobu, S. Mori, T. Shimoda, T. Mitani, H. Shimotani, N. Yoshimoto, S. Ogawa, Y. Iwasa, *Nat. Mater.* **2004**, *3*, 317.
[26] A. Ulman, *Chem. Rev.* **1996**, *96*, 1533.
[27] P. E. Laibinis, G. M. Whitesides, D. L. Allara, Y.-T. Tao, A. N. Parikh, R. G. Nuzzo, *J. Am. Chem. Soc.* **1991**, *113*, 7152.
[28] C. Kittel, *Solid State Physics*, 5th ed., Wiley, New York **1976**.
[29] C. A. Alves, M. D. Porter, *Langmuir* **1993**, *9*, 3507.
[30] *Handbook of Chemistry and Physics*, 75th ed. (Ed: D. R. Lide), CRC Press, Boca Raton, FL, USA **1995**.
[31] a) P. W. M. Blom, M. J. M. de Jong, J. J. M. Vleggaar, *Appl. Phys. Lett.* **1996**, *68*, 3308. b) P. W. M. Blom, M. J. M. de Jong, C. T. H. F. Liedenbaum, *Polym. Adv. Technol.* **1998**, *9*, 390.
[32] a) H. Tillmann, H.-H. Hörhold, *Synth. Met.* **1999**, *101*, 138. b) A. J. Breeze, Z. Schlesinger, S. A. Carter, H. Tillmann, H.-H. Hörhold, *Sol. Energy Mater. Sol. Cells* **2004**, *83*, 263.
[33] S. C. Veenstra, W. J. H. Verhees, J. M. Kroon, M. M. Koetse, J. Sweelssen, J. J. A. M. Bastiaansen, H. F. M. Schoo, X. Yang, A. Alexeev, J. Loos, U. S. Schubert, M. M. Wienk, *Chem. Mater.* **2004**, *16*, 2503.
[34] The electron current in a conventional polymer/polymer PV cell based on a PEDOT/PSS bottom contact and a LiF/Al top contact can differ from the electron-only current measured in Figure 3B, since the accumulation of holes might alter the electron transport.
[35] C. Naud, P. Calas, H. Blancou, A. Commeyras, *J. Fluorine Chem.* **2000**, *104*, 173.
[36] C. J. Neef, J. P. Ferraris, *Macromolecules* **2000**, *33*, 2311.
[37] W. N. Hansen, G. J. Hansen, *Surf. Sci.* **2001**, *481*, 172.

